

Interactions between slow and fast conductances in the Huber/Braun model of cold-receptor discharges

H.A. Braun^{a,*}, M.T. Huber^b, N. Anthes^a, K. Voigt^a, A. Neiman^c,
X. Pei^c, F. Moss^c

^a*Institute of Physiology, University of Marburg, Deutschhausstr. 2, D-35037 Marburg, Germany*

^b*Department of Psychiatry and Psychotherapy, University of Marburg, Rudolf-Buttmannstr. 8,
D-35033, Marburg, Germany*

^c*Center for Neurodynamics, University of Missouri, St. Louis, MO, USA*

Accepted 13 January 2000

Abstract

Transitions between different types of impulse patterns, according to experimentally recorded cold-receptor discharges, can successfully be mimicked with a minimal Hodgkin–Huxley-type simulation, here referred to as the Huber/Braun cold-receptor model. The model consists of two sets of simplified de- and repolarizing ionic conductances responsible for spike generation and slow-wave potentials, respectively. Over a broad temperature range, spike patterns are determined by the periodicity of subthreshold oscillations. At low temperatures, however, the periodicity of the pattern is destroyed and then appears again but with different patterns of different rhythmicity. We demonstrate that these complex transitions originate from the interactions between slow-wave and spike-generating currents. © 2000 Elsevier Science B.V. All rights reserved.

Keywords: Low-dimensional dynamics; Cold-receptor neuron model; Subthreshold oscillations; Bursts; Bifurcations

1. Introduction

Cold receptors are exceptional in so far as they exhibit a broad variety of different types of impulse patterns which systematically change depending on the temperature stimulus [2,7]. Such impulse pattern modifications have been simulated in computer

* Corresponding author. Tel.: 0049-6421-28-2305; fax: 0049-6421-28-6967.

E-mail address: braun@mail.uni-marburg.de (H.A. Braun).

models using rather general approaches [10] or directly referring to cold receptor discharges [6,17].

We here examine the characteristics of a recently developed model which is based on a simplified Hodgkin–Huxley-type approach, consisting of two sets of ionic conductances for subthreshold slow-wave oscillations and spike generation [6]. According to the cold-receptor discharges, the model produces regular burst activity over a broad temperature range due to slow oscillation cycles each triggering a group of impulses during its subthreshold phase. An additional stochastic term, i.e. noise, has to be introduced not only to obtain more realistic simulations but also to account for a specific type of experimentally recorded pattern which cannot be seen in purely deterministic simulations. Such noisy patterns are typical also of other types of thermosensitive receptors [7,9] as well as of many neurons in the brain [1,16,18] and have been analyzed in detail also in simulation studies [16] some of them using a slightly modified approach of the model described here [14,15].

However, there is another type of irregular pattern which seems mainly to be caused not by noise but essentially to originate from low-dimensional dynamics of the transduction system. In the experimental data this is indicated with recently developed methods for searches for stable and unstable manifolds in noisy neuronal data files [3,4,8,19]. In the model, the transitions to “chaotic” dynamics can clearly be seen in deterministic simulation runs which very recently have been analyzed in more detail with regard to bifurcation structures and the topological features [5,11,13]. Here, we also will focus on this particular type of pattern to examine the dynamical interactions from which these irregular dynamics arise in otherwise regularly operating oscillators.

In the next section, we first will briefly describe the model and then illustrate the principle characteristics of temperature scaling. In the main section, we will elucidate how the spike-generating mechanisms interfere with the subthreshold oscillations and, under certain conditions, can completely destroy the regular oscillatory behavior. We will conclude with a discussion especially considering the implications of our results for spike-pattern analysis in experimental data.

2. The Huber/Braun cold-receptor model

The Huber/Braun cold-receptor model has previously been described in detail [6,5,11,13]. In brief, it consists of two minimal sets of ionic conductances, each including simplified de- and repolarizing Hodgkin–Huxley-type currents with sigmoidal steady-state activation kinetics. For simplicity, inactivation is neglected. The current sets operate at different voltage levels and time scales. High threshold, fast activating currents are for spike generation (marked by indices d and r). Low threshold, slowly activating currents generate subthreshold potential oscillations (indices sd and sr). Including a leakage conductance g_1 and membrane capacitance C_M , the membrane potential V is given by

$$C_M dV/dt = f(V) = -g_1(V - V_1) - \alpha(I_d + I_r) - \beta(I_{sd} + I_{sr}). \quad (1)$$

The constants α and β are used to alter the extent to which the two current sets for spike generation and oscillation, respectively, contribute to the behavior of the system.

The voltage-dependent currents are calculated from the following equations ($i = d, r, sd, sr$):

$$I_i = \rho g_i a_i (V - V_i), \quad (2)$$

$$a_{i\infty} = 1/(1 + \exp(-s_i(V - V_{0i}))). \quad (3)$$

$$da_i/dt = \phi(a_{i\infty} - a_i)/\tau_i, \quad (4)$$

with V_i the equilibrium (Nernst) potentials, g_i the conductances and V_{0i} the half-activation potentials. The slopes of the steady-state activation variables, $a_{i\infty}$, are s_i , and the τ_i are the voltage independent time constants used for calculation of the actual value a_i .

Exceptions are: (a) instantaneous activation of the fast depolarizing current and (b) direct coupling of the slow repolarizing current to the slow depolarizing current according to

$$(a) a_d = a_{d\infty}, \quad (b) da_{sr}/dt = \phi(-\eta I_{sd} - ka_{sr})/\tau_{sr} \quad (5)$$

with η as coupling constant and k as a relaxation factor.

The temperature dependencies are obtained with scaling parameters ρ and ϕ for the maximum conductances and the time constants, respectively (T : temperature, T_0 : reference temperature):

$$\rho = 1.3^{(T - T_0)/10}, \quad \phi = 3.0^{(T - T_0)/10}. \quad (6)$$

Gaussian white noise is implemented according to the Box–Mueller algorithm (see [12]):

$$g_w = (-4d \, dt \ln(a))^{1/2} \cos(2\pi b) \quad (7)$$

with a, b random numbers between 0 and 1. Noise intensity is adjusted by the dimensionless parameter d and directly added to the membrane potential [12]:

$$V_{t+dt} = V_t + f(V) dt + g_w. \quad (8)$$

3. Temperature characteristics of noisy and deterministic simulations

Our computer model exhibits systematic temperature dependencies that, in noisy simulations, successfully mimic the major characteristics of the experimental data (Fig. 1A). At mid-temperatures (e.g. 16°C and 24°C in Fig. 1A), there are strong potential oscillations which generate regular burst discharges forming two distinct bands of inter-spike intervals. Towards higher temperatures, the oscillations are accelerated which simultaneously reduces the number of spikes per burst until the pattern changes to single-spike activity with an increasing number of oscillations without spike-generation (so-called “skippings”) leading to multimodal interval distributions (above about 30°C). This is the situation where noise is assumed to play an

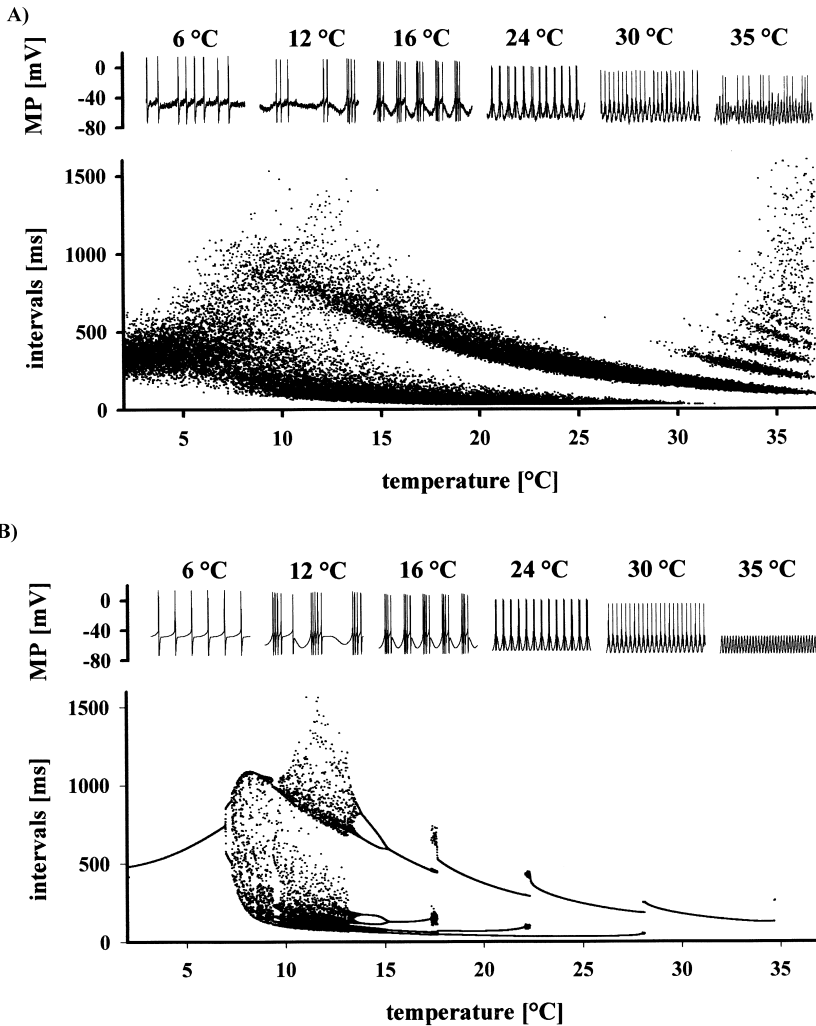


Fig. 1. Examples of voltage traces (upper diagrams, MP: membrane potential) and bifurcation plots of interspike intervals (lower diagrams) during temperature scaling of the Huber/Braun model under noisy (A) and deterministic (B) conditions. The noisy simulation ($a, d = 0.5$) fairly well mimicks experimental cold-receptor data with continuous transitions from irregular firing to bursting and "skippings". The deterministic simulation ($b, d = 0$) shows abrupt transitions between different dynamical states (without a range of "skippings") and elucidate details of complex bifurcations occurring at the transitions from tonic firing to burst discharges at low temperatures.

essential role: spike generation is clearly phase-locked to the underlying oscillations, but noise determines the threshold crossings and hence the times at which spikes are generated. The importance of noise seems also to increase towards the lower extreme of the temperature range with more irregular spike patterns and weakened

oscillations. Here, however, the broadened interval bands merge and phase-locking and periodicities of the pattern disappear until nearly Gaussian interval distributions are seen.

The deterministic model elucidates particular details that are concealed in the noisy simulations (Fig. 1B). Starting at high temperatures, the behavior of the model suddenly changes from completely subthreshold oscillations to regular single-spike discharges without a range of “skippings” in between (below and near 35°C). Towards lower temperatures, there are several abrupt transitions from period-one to period-four whenever the number of spikes per oscillation cycle increases. However, at a certain temperature (15°C), a rapidly increasing number of bifurcations occurs followed (at about 13°C) by a range of chaotic patterns with several periodic windows in between. At still lower temperatures (below about 7.5°C) the chaotic dynamics again disappear and are replaced by regular (period-one) single-spike activity.

Altogether, over a broad temperature range (above about 15°C) the discharge patterns are clearly determined by the slow-wave oscillations which trigger one or more impulses during their depolarising phases. This holds true for both deterministic and noisy simulations with the exception that noise can induce spiking as well as skipping around the onset of period-one activity at about 35°C. In the regular bursting range, noise is without qualitative effects on the pattern but mainly smoothens the deterministically abrupt transitions. In the chaotic regime noise destroys the fine structure of the bifurcations. However, the noisy simulations still show the same qualitative differences between the pattern below and above this deterministically chaotic regime (e.g., burst discharges at 16°C and tonic firing at 6°C) as do the deterministic simulations.

4. Interactions of slow-wave oscillations and spike-generating mechanisms

Over the entire temperature range, spike generation depends on the presence of slow-wave currents. With $\beta = 0$ the model would come to rest at a stable membrane potential without any spikes. In contrast, without spikes ($\alpha = 0$) slow oscillations are present at all temperatures with systematic, monotonic alterations of the oscillation period and some minor modifications of amplitude and shape in the dependence on temperature scaling. Examples of such slow-wave potentials without spike-generating mechanisms are plotted in the lower traces of Fig. 2. For comparison, the membrane potentials of the complete model, including the spikes, as already shown in Fig. 1B, are plotted in the upper traces.

For the examples at 16°C and higher temperatures, the situation is easy to understand. The subthreshold currents introduce slow waves also at the spike generator with action potentials riding on their crest until the depolarization reaches a certain value and remains at or above it for a certain time. The complete system, compared to the oscillations alone, appears to be somehow accelerated, which might result from faster activation of the slow depolarizing current due to spike repolarization.

But these are only minor effects compared to the situation at lower temperatures, which we now will consider in more detail. At 12°C, despite regular oscillations of the

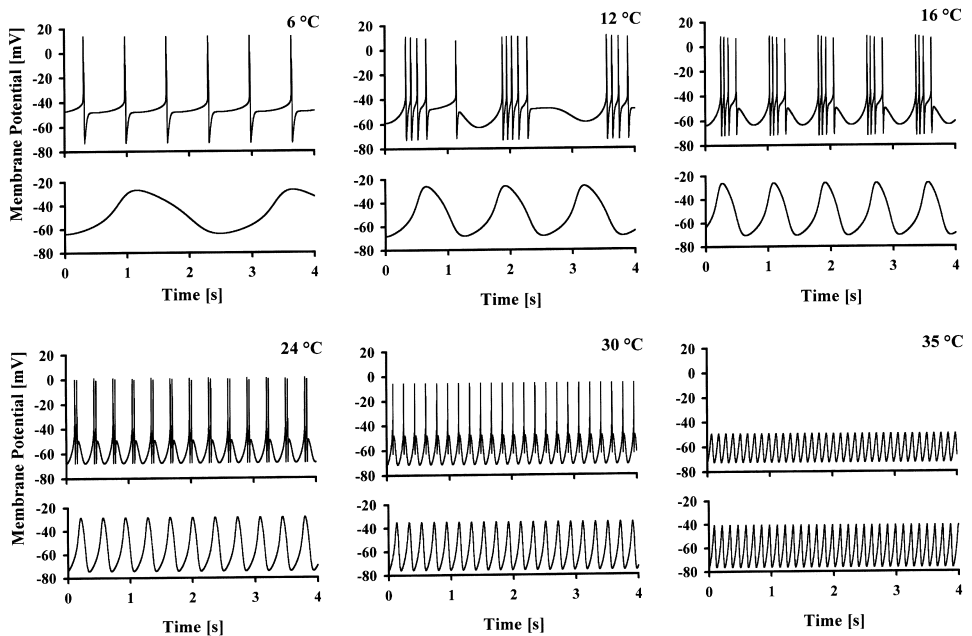


Fig. 2. Examples of voltage traces of deterministic simulations at different temperatures (see Fig. 1). Upper traces are from the complete model. Lower traces show slow-wave potentials without spike-currents ($\alpha = 0$). At highest temperature (35°C) the oscillations of the deterministic system remain subthreshold. At mid-temperatures (16°C, 24°C, 30°C) the spikes are generated in the rhythm of the slow-wave potentials with only slight acceleration by the spikes. At low temperatures (6°C, 12°C) the slow-wave potentials are destroyed with the occurrence of spikes.

isolated slow-wave currents, the coupled system has changed to chaotic dynamics. Only some remnants of the slow waves can still be seen in the spike train during longer intervals. At still lower temperatures (6°C), however, nothing seems to be left of the slow oscillations, although we know that the fast currents alone are not able to generate spikes. Hence, some qualitatively new behavior seems to appear depending on the generation of spikes. For further examination of these effects, we continuously reduced the spike amplitudes of our model by scaling the parameter α . We expected that the slow oscillations, which are clearly seen at $\alpha = 0$, but are completely absent at $\alpha = 1$, should become visible at a certain value in between. The result is shown in the bifurcation plot of Fig. 3, where α is linearly scaled down from 1.0 to 0.3.

The bifurcation plot starts at the period-one situation at 6°C with $\alpha = 1$ without recognizable oscillations. Indeed, it ends with rhythmic burst generation, and the bursts are mediated by the clearly visible slow-wave oscillations. These oscillations, however, do not gradually develop. Instead, the system again passes through the complete bifurcation structure similar to the behavior observed in the case of temperature scaling. Even the specific effects of the homoclinic bifurcation, as described by Braun et al. [5] and Feudel et al. [11] can be seen.

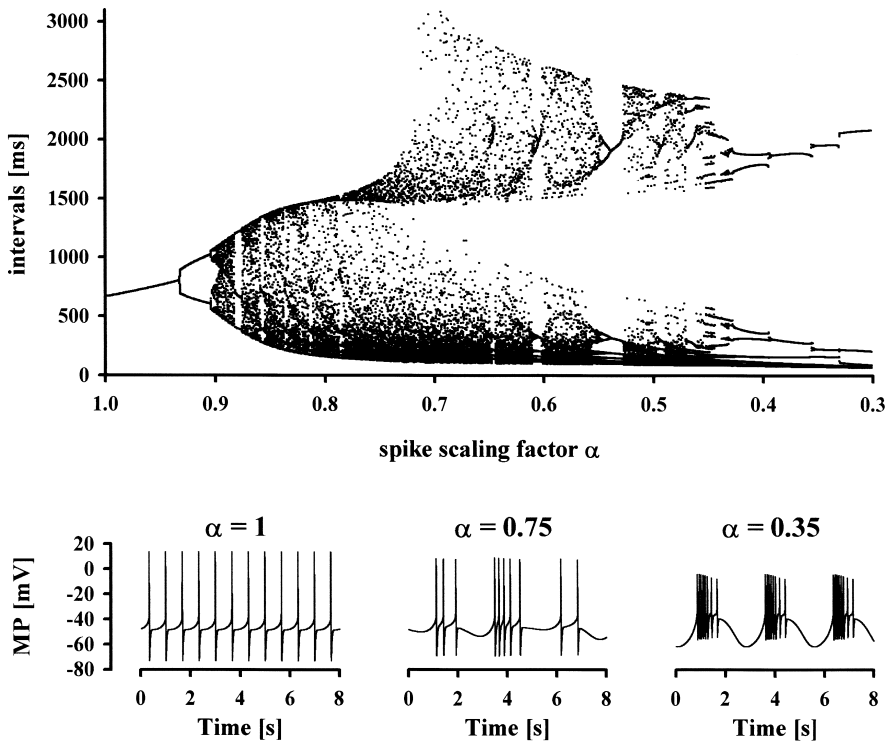


Fig. 3. Bifurcation plot of the interspike intervals during linearly reduced spike amplitudes according to the spike-scaling factor α (upper trace) and examples of voltage traces (lower traces, MP: membrane potential). With reduced α , the pattern changes from regular tonic firing (period-one discharges) to regular bursting thereby passing a range of bifurcations and chaotic dynamics similar to temperature scaling (see Fig. 1).

5. Conclusions

The results have shown that completely identical mechanisms of slow-wave oscillations can give rise to qualitatively totally different spike patterns depending on the amplitude of the spikes which they are generating. The patterns can change from burst discharges to tonic firing whereby, most remarkably, a range of low-dimensional impulse activity is passed.

With such pronounced alterations, of course, it can be expected that the information carried by the impulse trains also significantly changes. This can have essential implications for neuronal information processing, since most external stimuli (neurotransmitters, hormones, etc.) interfere with the ionic conductances thereby altering the amplitude of the spikes. Indeed, these effects are not necessarily due to the spike conductances alone, but it is likely that similar effects could be seen with alterations of the slow-wave currents. Here we assume that the transitions do not depend only on

the absolute values of the ionic currents, but on the relation between the currents of the two subsystems.

Finally, coming back again to the temperature dependencies, it should be noticed that there are two different types of transitions from tonic firing to bursting. One is seen at high temperatures in the course of a temperature decrease, where the dynamical behavior shows no qualitative change. What happens is only the addition of one more spike during the slow-wave cycle, as it occurs several times more in the bursting range up to a number of four. The other type of transition is seen at low temperature, in the course of a slow temperature increase. The interval distribution bifurcates from period-one to period-two, period-four, etc., exhibiting low-dimensional dynamical behaviors (for example, transitions from nodes to foci) followed by chaotic impulse generation before a region of regular burst discharges is attained. This can be seen with temperature scaling as well as with scaling of the spike amplitudes. Therefore, it might be suspected that this type of transition — from tonic firing to bursts in general — always passes through a range of chaotic dynamics. Remarkably, indications of these dynamical behaviors at transitions from tonic firing to burst discharges have also been seen in experimental data files recorded from cold receptors as well as from other neurons [3,4].

Acknowledgements

This work is supported by the Volkswagen-Stiftung and the Kempkes-Stiftung, Marburg. M.T. Huber is supported by the Gesellschaft für Neurobiologische Forschung und Therapie, A. Neiman by the Fetzer Institute, F. Moss by the US Office of Naval Research, and X. Pei by the US Department of Energy. We wish to thank W. Braun and B. Eckhardt, Physics Dept., Marburg, for stimulating discussions.

References

- [1] A. Alonso, K. Klink, Differential electroresponsiveness of stellate- and pyramidal-like cells of medial entorhinal cortex layer II, *J. Neurophysiol.* 70 (1993) 128–143.
- [2] H.A. Braun, H. Bade, H. Hensel, Static and dynamic discharge patterns of bursting cold fibers related to hypothetical receptor mechanisms, *Pflügers Arch.* 386 (1980) 1–9.
- [3] H.A. Braun, M. Dewald, K. Schäfer, K. Voigt, X. Pei, K. Dolan, F. Moss, Low-dimensional dynamics in sensory biology 2: facial cold receptors of the rat, *J. Comput. Neurosci.* 7 (1999) 17–32.
- [4] H.A. Braun, M. Dewald, K. Voigt, M. Huber, X. Pei, F. Moss, Finding unstable periodic orbits in electroreceptors, cold receptors and hypothalamic neurons, *Neurocomputing* 26–27 (1999) 79–86.
- [5] W. Braun, B. Eckhardt, H.A. Braun, M.T. Huber, Phase space structure of a thermoreceptor, *Phys. Rev. E*, submitted for publication.
- [6] H.A. Braun, M.T. Huber, M. Dewald, K. Schäfer, K. Voigt, Computer simulations of neuronal signal transduction: the role of nonlinear dynamics and noise, *Int. J. Bifurc. Chaos* 8 (1998) 881–889.
- [7] H.A. Braun, K. Schäfer, H. Wissing, H. Hensel, Periodic transduction processes in thermosensitive receptors, in: W. Hamann, A. Iggo (Eds.), *Sensory Receptor Mechanisms*, World Scientific, Singapore, 1984, pp. 147–156.

- [8] H.A. Braun, K. Schäfer, K. Voigt, R. Peters, F. Bretschneider, X. Pei, L. Wilkens, F. Moss, Low-dimensional dynamics in sensory biology 1: thermally sensitive electroreceptors of the catfish, *J. Comput. Neurosci.* 4 (1998) 335–347.
- [9] H.A. Braun, H. Wissing, K. Schäfer, M.C. Hirsch, Oscillation and noise determine signal transduction in shark multimodal sensory cells, *Nature* 367 (1994) 270–273.
- [10] T.R. Chay, Y.S. Fan, Y.S. Lee, Bursting, spiking, chaos, fractals and universality in biological rhythms, *Int. J. Bifurc. Chaos* 5 (1995) 595–635.
- [11] U. Feudel, A. Neiman, X. Pei, W. Wojtenek, H.A. Braun, M.T. Huber, Homoclinic bifurcations in a Hodgkin–Huxley model of thermally sensitive neurons, *Chaos*, in press.
- [12] R.F. Fox, I.R. Gatland, R. Roy, G. Vemuri, Fast, accurate algorithm for numerical simulation of exponentially correlated colored noise, *Physical Rev. A* 38 (1988) 5938–5940.
- [13] R. Gilmore, X. Pei, F. Moss, Topological analysis of chaos in neural spike train bursts, *Chaos* 9 (1999) 812–817.
- [14] M.T. Huber, H.A. Braun, K. Voigt, J.C. Krieg, Computational properties of intrinsic subthreshold oscillations, in: J. Bower (Ed.), *Computational Neuroscience: Trends in Research 1998*, Plenum Press, New York, 1998, pp. 197–202.
- [15] M.T. Huber, J.C. Krieg, M. Dewald, K. Voigt, H.A. Braun, Stimulus sensitivity and neuromodulatory properties of noisy intrinsic neuronal oscillators, *Biosystems* 48 (1998) 95–104.
- [16] R.R. Llinas, A.A. Grace, Y. Yarom, In vitro neurons in mammalian cortical layer 4 exhibit intrinsic oscillatory activity in the 10–50 Hz frequency range, *Proc. Natl. Acad. Sci. USA* 88 (1991) 897–901.
- [17] A. Longtin, K. Hinzer, Encoding with bursting, subthreshold oscillations and noise in mammalian cold receptors, *Neural Comput.* 8 (1995) 215–255.
- [18] D. Pare, H.C. Pape, J. Dong, Bursting and oscillating neurons of the cat basolateral amygdaloid complex in vivo: electrophysiological properties and morphological features, *J. Neurophysiol.* 74 (1995) 1179–1191.
- [19] X. Pei, F. Moss, Characterization of low-dimensional dynamics in the crayfish caudal photoreceptor, *Nature* 379 (1996) 618–621.